



34 **Abstract**

35 Bias correction of climate variables is a standard practice in Climate Change Impact (CCI) studies.
36 Various methodologies have been developed within the framework of quantile mapping. However,
37 it is well known that quantile mapping may significantly modify the long term statistics due to the
38 time dependency that the temperature bias. Here, a method to overcome this issue without
39 compromising the day to day correction statistics is presented. The methodology separates the
40 model temperature signal into a normalized and a residual component relatively to the molded
41 reference period climatology, in order to adjust the biases only for the former and preserve intact
42 the signal of the later. The results show that the adoption of this method allows for the preservation
43 of the originally modeled long-term signal in the mean, the standard deviation and higher and
44 lower percentiles of temperature. The methodology is tested on daily time series obtained from
45 five Euro CORDEX RCM models, to illustrate the improvements of this method.

46

47

48

49

50

51

52

53

54

55

56

57

58

59

60

61

62

63

64

65

66

67 **Keywords:** temperature, trend preservation, moment preservation, statistical bias correction,



68 1 Introduction

69 Climate model output consist the primary source of information used to quantify the effect of the
70 foreseen anthropogenic climate change on natural systems. One of the most common and
71 technically sound practices in Climate Change Impact (CCI) studies is to calibrate impact models
72 using the most suitable observational data and then to replace them with the climate model data
73 in order to assess the effect of potential changes in the climate regime. Often, raw climate model
74 data cannot be used in CCI models due to the presence of biases in the representation of regional
75 climate (Christensen et al., 2008; Haerter et al., 2011). In fact, hydrological CCI studies outcome
76 have been reported to become unrealistic without a prior adjustment of climate forcing biases
77 (Hansen et al., 2006; Harding et al., 2014; Sharma et al., 2007). These biases may be attributed
78 to a number of sources such as the imperfect representation of the physical processes within the
79 model code and the coarse spatial resolution that do not permit the accurate representation of
80 small-scale processes. Furthermore, in some cases, climate model tuning for global projections
81 focuses on the adequate representation of feedbacks between processes and hence the realistic
82 depiction of a variable, such as temperature, against observations is sidelined (Hawkins et al.,
83 2016).

84 A number of statistical bias correction methods have been developed and successfully applied in
85 CCI studies (e.g. Grillakis et al., 2013; Haerter et al., 2011; Ines and Hansen, 2006; Teutschbein
86 and Seibert, 2012). Their main task is to adjust the statistical properties of climate simulations to
87 resemble those of observations, in a common climatological period. A commonly used type of
88 procedure to accomplish this is using a Transfer Function (TF) which minimizes the difference
89 between the cumulative density function (CDF) of the climate model output and that of the
90 observations, a process also referred to as quantile mapping. As a result of quantile mapping, the
91 reference (calibration) period's adjusted data are statistically closer, and sometimes near-identical
92 to the observations. Hence the statistical outcome of an impact model run using observational
93 data is likely to be reproduced by the adjusted data. The good performance of statistical bias
94 correction methods in the reference period is well documented (Grillakis et al., 2011; Grillakis et
95 al., 2013; Ines and Hansen, 2006; Papadimitriou et al., 2015). The procedure however overlooks
96 the time dependency of the biases, i.e the unequal effect of the TF to the varying over time CDF.
97 An indicative example is presented in Figure 1 where modeled temperature data have a mean
98 bias of 2.49 °C in the reference period (Figure 1a) relatively to the observations. This mean bias
99 is expressed by the average horizontal distance between the TF and the bisector of the central
100 plot. The left histogram illustrates the reference period modeled data for 1981-2010. The
101 histogram at the bottom is derived from observational data. The histogram on the right is derived



102 from a moving 30-year period between 1981 and 2098. Finally the rightmost histogram shows the
103 difference between the reference period and the moving 30-year period. The red mark shows the
104 theoretical change in the average correction applied by the TF, due to the changes in the projected
105 temperature histogram. Hence, the average correction applied for the 2068-2097 period reaches
106 3.85 °C, significantly higher than the reference period's bias (Figure 1b). The time-dependency of
107 the correction magnitude introduces a long term signal distortion in the corrected data. In the
108 quantile mapping based correction methodologies in which the TF distance from the bisector is
109 variable, this effect is unavoidable. Nevertheless, in cases where the TF retains a relatively
110 constant distance to the bisector (i.e. parallel to the bisector), the trend of the corrected data
111 remains similar to the raw model data regardless of the temporal change in the model data
112 histogram.

113

114

115 Based on the previous example, the time extrapolation of the TF use is regarded as a leap of faith
116 that may lead to a false certainty about the robustness of the adjusted projection. This may
117 significantly change the original model derived long-term trend or other higher moments of the
118 climate variable statistics that eventually change the long-term signal of the climate variable. In
119 their work on distribution based scaling (DBS) bias correction, Olsson et al. (2015) showed that
120 their methodology might alter the long-term temperature trends, attributing the phenomenon in
121 the severity of the biases in the mean or the standard deviation between the uncorrected
122 temperatures and the observations. Maraun, (2016) discuss on whether the change in the trend
123 is a desired feature of bias correction, concluding that it is case specific, depending on the
124 skillfulness of a model to simulate the correct long term signal. In the case of CCI studies this
125 implies that climate model data is assessed for its skill to well represent the trend, which does not
126 consist a common practice. A possible but indirect solution to this is described in Maurer and
127 Pierce, (2014) who study the change in precipitation trend over an ensemble of atmospheric
128 general circulation model (AGCM). They concluded that, while individual quantile mapping
129 corrected AGCM data may significantly modify the signal of change, a relatively large ensemble
130 estimation diminished the problem due to the cancel out of the individual model trend changes.
131 Li et al. (2010) present a quantile mapping method to adjust temperature biases taking into
132 account the differences of the future and reference period distributions. A drawback of the method
133 is that the difference between the two periods' distributions depends on the future period length.
134 In their work, Hempel et al. (2013) propose a methodology to resolve the trend changing issue,



135 by preserving the absolute changes in monthly temperature, and relative changes in monthly
136 values of precipitation. A conceptual drawback of this approach that it maps anomalies instead
137 of absolute values, indicating that specific correction values are attached to each temperature
138 anomaly. A similar additive for temperature and multiplicative for precipitation approach was also
139 followed by (Pierce et al., 2015).

140 In this study, we present a methodology to conserve the long term statistics of the climate model
141 data in quantile mapping. The methodology considers the separation of the temperature signal
142 relatively to the raw data reference period, producing a normalized and a residuals data stream.
143 The residuals include the gradual changes in the signal and potential non-stationary changes.
144 The quantile mapping bias correction is then applied to the normalized time series. Finally, the
145 residual components are again merged to the bias corrected time series to form the finally
146 corrected time series. The methodology is tested along with a generalized version of the Multi-
147 segment Statistical Bias Correction (MSBC) quantile mapping methodology (Grillakis et al., 2013).
148 The methodology takes the form of a pre- and post-processing module that can be applied along
149 with different statistical bias correction methodologies.

150

151 **2 Methods**

152 **2.1 Residual separation**

153 The statistical difference of each individual year's simulated data, comparing to the average
154 reference period simulated data is identified as residuals. These are estimated between the CDF
155 of each year's modeled climate data and the CDF of the entire reference period of the model data.
156 Let S_R be the reference period model data and S_i the climate data for year i , then the normalized
157 data S_i^N for year i are estimated by transferring each year's data onto the average reference
158 period CDF through a transfer function TF_{S_i} estimated annually. This can be formulated as Eq.(1).

159

$$S_i^N = TF_{S_R}^{-1} \left(TF_{S_i} (S_i) \right) \quad \text{Eq. (1)}$$

160

161 The difference between the original model data S_i and the normalized data S_i^N are the residual
162 components S_i^D of the time series (Eq. (2)).

163

$$S_i^D = S_i - S_i^N \quad \text{Eq. (2)}$$

164



165 The original model data S_i can be reproduced by adding back the residuals S_i^D to the normalized
166 data S_i^n . After the separation, the normalized climate model data are statistically bias corrected
167 following a suitable methodology. The residuals are preserved in order later to be added again to
168 the bias corrected time series. We refer to the described method as Normalization Module (NM)
169 to hereafter lighten the nomenclature of the paper. The normalization procedure is performed in
170 annual basis, as it consists an obvious periodicity to use in the case of temperature, even if it is
171 not so well defined in tropics. The underlying assumption of the NM procedure is that it assumes
172 that there are no major changes in the reference period data, an assumption that can hardly fall
173 short due to the usually short length of the reference period.

174

175 **2.2 Bias correction**

176 Here, the NM is applied along with a modification of the MSBC algorithm that is presented in
177 Grillakis et al. (2013). This methodology follows the principles of quantile mapping correction
178 techniques and was originally designed and tested for GCM precipitation adjustment. The method
179 partitions the CDF data into discrete segments and an individual quantile mapping correction is
180 applied to each segment, achieving a better fitted transfer function. Here the methodology is
181 modified to use linear functions instead of the gamma functions used in the original methodology,
182 in order to facilitate potential negative temperature values but also as a known technique in
183 quantile mapping, as it has also been used elsewhere (Thiemeßl et al., 2011). An indicative
184 example is shown in Figure 2, where the CDFs are split into discrete segments and linear
185 functions are fit to each of them. In Figure 2, p symbolizes the cumulative probability and s is the
186 slope of the linear function. Then the corrected temperature for each temperature value of the
187 specific segment is estimated as in Eq. (3).

188

$$T_{corr}^n = s_{obs}^n * \left(\frac{T_{raw}^n - b_{raw}^n}{s_{raw}^n} \right) + b_{obs}^n \quad \text{Eq. (3)}$$

189

190 The optimal number of the segments is estimated by Schwarz Bayesian Information Criterion
191 (SBIC) to balance between complexity and performance. Additionally, the upper and lower edge
192 segments are explicitly corrected using the average difference between the reference period of
193 the raw model data and the observations (Figure 2 ΔT). This provides robustness, avoiding
194 unrealistic temperature values at the edges of the model CDF. The bias correction methodology
195 modification has been already used in the Bias Correction Intercomparison Project (BCIP) (Nikulin



196 et al., 2015), while produced adjusted data have been used in a number of CCI studies
197 (Daliakopoulos et al., 2016; Grillakis et al., 2016; Koutroulis et al., 2016; Papadimitriou et al.,
198 2016). As the MSBC methodology belongs to the parametric quantile mapping techniques, it
199 shares their advantages and drawbacks. A comprehensive shakedown of advantages and
200 disadvantages of quantile mapping in comparison to other methods can be found in Maraun et al.
201 (2010) and Themeßl et al. (2011). A step by step example of the multisegment correction
202 procedure is provided in Appendix A of (Grillakis et al., 2013).

203

204 **3 Case study area and data**

205 To examine the effect of NM on the bias correction on a timeseries, the Hadley Center Central
206 England Temperature (HadCET - Parker et al., 1992) observational dataset was considered to
207 adjust the simulated output from the earth system model MIROC-ESM-CHEM (Hasumi and
208 Emori, 2004) historical emissions run between 1850 and 2005 for Central England. This particular
209 case study was chosen due to the large observational record (the longest instrumental record of
210 temperature in the world) that is available for central England, i.e. the triangular area of the United
211 Kingdom enclosed by Lancashire, London and Bristol. Discussion about dataset related
212 uncertainties can be found in Parker et al., (1992) and Parker and Horton (2005). The Klemes
213 (1986) split sample test methodology was adopted for verification. Split sample is the most
214 common type of test used for the validation of model efficiency. The methodology considers two
215 periods of calibration and validation, between the observed and modeled data. The first period is
216 used for the calibration, while the second period is used as a pseudo-future period in which the
217 adjusted data are assessed against the observations. A drawback of the split sample test in bias
218 correction validation operations is that the remaining bias of the validation period is a function of
219 the bias correction methodology deficiency and the model deficiency itself to describe the
220 validation period's climate, in aspects that are not intended to be bias corrected. That said, a
221 skillful bias correction method should deal well in that context, as model "democracy" (Knutti,
222 2010), i.e. the assumption that all model projections are equally possible, is common in CCI
223 studies with little attention to be given to the model selection. In the specific application and in
224 order to resemble a typical CCI study, data between 1850 and 1899 serve as calibration period,
225 while the rest of the data between 1900 and 2005 is used as pseudo-future period for the
226 validation. Finally, the bias correction results of the two procedures, with (BC-NM) and without
227 (BC) the normalization module, were compared against the validation period observations.

228 Furthermore, to expand the methodology assessment in regional scale, the split sample test is
229 adopted to assess the efficiency of the two procedures in a pan European scale. In order to scale



230 up the split sample test, the k-fold cross validation test (Geisser, 1993) is employed. The
231 procedure has been proposed for evaluating the performance of bias correction procedures in
232 (Maraun, 2016). In k-fold cross validation test, the data is partitioned into k equal sized folds. Of
233 the k folds, one subsample is retained each time as the validation data for testing the model, and
234 the remaining k-1 subsamples are used as calibration data. In a final test, the procedures are
235 applied on a long-term transient climate projection experiment to assess their effect in the long-
236 term attributes of the temperature in a European scale application.

237 Temperature data from the European division of Coordinated Regional Downscaling Experiment
238 (CORDEX), openly available through the Earth System Grid Federation (ESGF), are considered.
239 Additional information about the Euro - CORDEX domain can be found on the CORDEX web
240 page (<http://wcrp-cordex.ipsl.jussieu.fr/>). Data from five RCM models (Table 1) with 0.44° spatial
241 resolution and daily time step between 1951-2100 are used. The projection data are considered
242 under the Representative Concentration Pathway (RCP) 8.5, which projects an 8.5 W m⁻² average
243 increase in the radiative forcing until 2100. The European domain CORDEX simulations have
244 been evaluated for their performance in previous studies (Kotlarski et al., 2014; Prein et al., 2015).
245 The EOBSv12 temperature data was used (Haylock et al., 2008). Discussion about the
246 applicability of EOBS to compare temperature of RCMs control climate simulations can be found
247 in Kyselý and Plavcová (2010). Figure 3 shows the 1951-2005 daily temperature average and
248 standard deviation for the five RCMs of Table 1. The RCMs' mean bias ranges between about -2
249 °C and 1 °C relatively to the EOBS dataset. The positive mean bias in all RCMs is mainly seen in
250 Eastern Europe, while the same areas exhibit negative bias in standard deviation. Some of the
251 bias is however attributed to the ability of the observational dataset to represent the true
252 temperature.

253 For the k-fold cross validation, the RCM data between 1951-2010 are split into 6 ten-year sections,
254 comprising a 6-fold, 5 RCM ensemble experiment of Figure 4. Each section is validated once by
255 using the rest five sections for the calibration. A total number of 30 tests are conducted using
256 each procedure.

257 For the transient experiment, the RCM data between 1951 and 2100 are considered, using the
258 1951-2010 as calibration to correct the 1951-2100 data.

259

260 **4 Results and discussion**

261 The results of the split sample test on the central England example are presented in Figure 5. In
262 Figure 5a the separation of the raw data performed by the NM into residuals and normalized raw
263 data in annual aggregates is shown. The normalized time series do not exhibit any trend or



264 significant fluctuation in the annual aggregates, since the normalization is performed at annual
265 basis, while the long-term trend and the variability is contained in the residual time series. In
266 Figure 5b, annual aggregates obtained via the above two procedures are compared to the raw
267 data and the observations. Results show that both procedures adjust the raw data to better fit the
268 observations in the calibration period 1850-1899. In the validation period, both procedures
269 produce similar results, but the BC-NM long-term linear trend is slightly lower than that of the BC
270 results. While the latter slope is closer to the observations' linear trend, the former is closer to the
271 raw data trend (Table 2). The persistence of the long-term trend is a desirable characteristic of
272 the NM procedure as the GCM long-term moments were not distorted by the correction. However,
273 the wider deviation of the BC-NM trend relatively to the BC depicts the skill of the GCM to simulate
274 the observations' respective trend. Figure 5c shows that the BC-NM output resemble the raw data
275 histograms in shape, but are shifted in their mean towards the observations. A small decrease in
276 the variability can also be observed in the BC-NM but consists a substantially smaller disturbance
277 relatively to the BC. The transfer of the mean with a simultaneous preservation of the larger part
278 of the variability consists a nearly idealized behavior for the adjusted data, as the distribution of
279 the annual temperature averages are retained after the correction. Similar results generated on
280 daily data (Figure 5d) show that both procedures adjust the calibration and validation histograms
281 in the same degree towards the observations. This can also be verified by the mean, the standard
282 deviation and the 10th and 90th percentile of the daily data (Table 2). An early concluding remark
283 about the NM is that it improved the long-term statistics of the adjusted data towards the climate
284 model signal, without sacrificing the daily scale quality of the correction.

285 In Figure 6, the results of the cross validation test of the bias correction on the Euro – CORDEX
286 data with and without the use of NM are shown, in terms of mean temperature. The mean of the
287 raw temperature data and the observations are respectively equal for their calibration and the
288 validation periods due to the design of the experiment. The bias correction results show that both
289 correction procedures with and without the NM, appropriately meet the needs in terms of the
290 mean value. The differences between the calibration and validation averages with the
291 corresponding observations show consistently low residuals. A significant difference between the
292 two tests is that the use of the NM increases the residuals due to the exclusion of the potentially
293 non-stationary components from the correction process. Nonetheless, the scale of the residuals
294 is considered below significance in the context of CCI studies, as it ranges only up to 0.035 °C.
295 The increased residuals of the NM are the trade off to the preservation of the model long-term
296 climate change signal, in the transient experiment. Figure 7 shows the long-term change in the
297 signal of the mean temperature, for the 10th and 90th percentiles (estimated on annual basis). The



298 trends are estimated by linear least square regression and are expressed in °C per century. The
299 use of the NM profoundly better preserved the long-term trend relatively to the raw model data in
300 all three cases. Without using the NM module, the distortion in the mean annual temperature trend
301 lies between -0.5 and 0.5 degrees per century, while the distortion in the 10th and 90th percentiles
302 are apparently more profound. Additionally, the northeastern Europe's 10th and 90th percentiles
303 reveal a widening of the temperature distribution when NM is not used. The widening is attributed
304 to the considerable negative trend in the p10 and the considerable positive p90 trend in the same
305 areas. The magnitude of the distortion is considerable and can potentially lead to CCI
306 overestimation. In contrast, with the use of NM the change in the trend is reduced in most of the
307 Europe's area.

308 The impact of NM on the standard deviation is also significant. Figure 8 shows the evolution of
309 the standard deviation of the daily data for each model, in the cases of raw data and the bias
310 corrected data using the BC and the BC_{NM}. The standard deviation is estimated for each grid point
311 and calendar year, and is averaged across the study domain. The results show that the standard
312 deviation of the adjusted data differ from the respective standard deviations of the raw data, in
313 both adjustment approaches. This is an expected outcome, as raw model data standard
314 deviations differ from the respective observed data standard deviation (Figure 8 d, e). However,
315 the standard deviation differences between BC_{NM} and the raw data (Figure 8 f) is significantly
316 more stable than that the respective differences from BC (Figure 8 g), meaning that the signal of
317 standard deviation is better preserved and does not inflate with time in the former case.
318 Additionally, the variation of the standard deviations time series exhibits lower fluctuations.

319

320 5 Conclusions

321 This study elaborates with the issue of the distortion of the long term statistics in quantile mapping
322 statistical bias correction relatively to the raw model data. An extra processing step is presented,
323 that can be applied along with quantile mapping statistical bias correction techniques. This step,
324 namely NM, splits the original data into two parts, a normalized one that is bias adjusted using
325 quantile mapping, and the residuals part that is added to the former after the bias correction. The
326 methodology is tested and validated from several points of view, leading to some key remarks
327 about its added value. First, it is shown that the use of the NM module results in the long-term
328 temperature trend preservation of the mean temperature change, but also of the trend in the
329 higher and lower percentiles. Furthermore, the examination of the standard deviation temporal
330 evolution show that is better retained relatively to the raw data, as the exclusion of the residuals
331 form the correction minimizes the inflation of the variance. Additionally, the inter-annual variability



332 of the raw data is preserved relatively to the simple quantile mapping, which consists an important
333 feature for climate impact studies that involve carbon cycle simulations (Rubino et al., 2016). As
334 a drawback, the corrected temperature using the NM is found to retain small portions of the
335 biases, which however is shown that is rather low to virtually affect an CCI study results.
336 The main advantage of the proposed method compared to other trend preserving methods is that
337 the preservation of the long-term mean trend is not the objective but rather an ineluctable
338 consequence of normalization before the bias correction process. Additionally the normalization
339 is performed in annual basis, hence the projection period results are not affected by the length of
340 the projection period. Nevertheless, it has to be stressed that a range of issues, such as the
341 disruption of the physical consistency of climate variables, the mass/energy balance and the
342 omission of correction feedback mechanisms to other climate variables (Ehret et al., 2012) have
343 not been addressed in this work despite the existence of methods that preserve consistency
344 between specific variables (Sippel et al., 2016). Finally, one should bare in mind that climate data
345 quality prime driver is the climate model skillfulness itself. Statistical post processing methods like
346 bias correction cannot add new information to the data but rather add usefulness to it, depending
347 on the needs of each application.

348

349 **Acknowledgements**

350 The research leading to these results has received funding from the HELIX project of the
351 European Union's Seventh Framework Programme for research, technological development and
352 demonstration under grant agreement no. 603864. We acknowledge the World Climate Research
353 Programme's Working Group on Regional Climate, and the Working Group on Coupled Modelling,
354 former coordinating body of CORDEX and responsible panel for CMIP5. We also thank the
355 climate modelling groups (listed in Table 1 of this paper) for producing and making available their
356 model output. Finally, we acknowledge the E-OBS data set from the ENSEMBLES EU-FP6
357 project (<http://ensembles-eu.metoffice.com>) and the data providers in the ECA&D project
358 (<http://www.ecad.eu>).

359

360 **References**

- 361 Christensen, J.H., Boberg, F., Christensen, O.B., Lucas-Picher, P., 2008. On the need for bias
362 correction of regional climate change projections of temperature and precipitation. *Geophys.*
363 *Res. Lett.* 35, L20709. doi:10.1029/2008GL035694
- 364 Daliakopoulos, I.N., Tsanis, I.K., Koutroulis, A.G., Kourgialas, N.N., Varouchakis, E.A., Karatzas,
365 G.P., Ritsema, C.J., 2016. The Threat of Soil Salinity: a European scale review. *CATENA*.



- 366 Ehret, U., Zehe, E., Wulfmeyer, V., Warrach-Sagi, K., Liebert, J., 2012. *HESS Opinions* “Should
367 we apply bias correction to global and regional climate model data?” *Hydrol. Earth Syst. Sci.*
368 16, 3391–3404. doi:10.5194/hess-16-3391-2012
- 369 Geisser, S., 1993. *Predictive inference*. CRC press.
- 370 Grillakis, M.G., Koutroulis, A.G., Papadimitriou, L. V, Daliakopoulos, I.N., Tsanis, I.K., 2016.
371 *Climate-Induced Shifts in Global Soil Temperature Regimes*. *Soil Sci.* 181, 264–272.
- 372 Grillakis, M.G., Koutroulis, A.G., Tsanis, I.K., 2013. Multisegment statistical bias correction of daily
373 GCM precipitation output. *J. Geophys. Res. Atmos.* 118, 3150–3162. doi:10.1002/jgrd.50323
- 374 Grillakis, M.G., Koutroulis, A.G., Tsanis, I.K., 2011. Climate change impact on the hydrology of
375 Spencer Creek watershed in Southern Ontario, Canada. *J. Hydrol.* 409.
376 doi:10.1016/j.jhydrol.2011.06.018
- 377 Haerter, J.O., Hagemann, S., Moseley, C., Piani, C., 2011. Climate model bias correction and the
378 role of timescales. *Hydrol. Earth Syst. Sci.* 15, 1065–1079. doi:10.5194/hess-15-1065-2011
- 379 Hansen, J.W., Challinor, A., Ines, A.V.M., Wheeler, T., Moron, V., 2006. Translating climate
380 forecasts into agricultural terms: advances and challenges. *Clim. Res.* 33, 27–41.
- 381 Harding, R.J., Weedon, G.P., van Lanen, H.A.J., Clark, D.B., 2014. The future for global water
382 assessment. *J. Hydrol.* 518, 186–193. doi:10.1016/j.jhydrol.2014.05.014
- 383 Hasumi, H., Emori, S., 2004. K-1 Coupled GCM (MIROC) Description K-1 model developers.
- 384 Hawkins, E., Sutton, R., Hawkins, E., Sutton, R., 2016. Connecting Climate Model Projections of
385 Global Temperature Change with the Real World. *Bull. Am. Meteorol. Soc.* 97, 963–980.
386 doi:10.1175/BAMS-D-14-00154.1
- 387 Haylock, M.R., Hofstra, N., Klein Tank, A.M.G., Klok, E.J., Jones, P.D., New, M., 2008. A
388 European daily high-resolution gridded data set of surface temperature and precipitation for
389 1950–2006. *J. Geophys. Res.* 113, D20119. doi:10.1029/2008JD010201
- 390 Hempel, S., Frieler, K., Warszawski, L., Schewe, J., Piontek, F., 2013. A trend-preserving bias
391 correction – the ISI-MIP approach. *Earth Syst. Dyn.* 4, 219–236. doi:10.5194/esd-4-219-
392 2013
- 393 Ines, A.V.M., Hansen, J.W., 2006. Bias correction of daily GCM rainfall for crop simulation studies.
394 *Agric. For. Meteorol.* 138, 44–53. doi:10.1016/j.agrformet.2006.03.009
- 395 Klemes, V., 1986. Operational testing of hydrological simulation models. *Hydrol. Sci. J.* 31, 13–
396 24. doi:10.1080/02626668609491024
- 397 Knutti, R., 2010. The end of model democracy? *Clim. Change* 102, 395–404. doi:10.1007/s10584-
398 010-9800-2
- 399 Kotlarski, S., Keuler, K., Christensen, O.B., Colette, A., Déqué, M., Gobiet, A., Goergen, K.,



- 400 Jacob, D., Lüthi, D., van Meijgaard, E., Nikulin, G., Schär, C., Teichmann, C., Vautard, R.,
401 Warrach-Sagi, K., Wulfmeyer, V., 2014. Regional climate modeling on European scales: a
402 joint standard evaluation of the EURO-CORDEX RCM ensemble. *Geosci. Model Dev.* 7,
403 1297–1333. doi:10.5194/gmd-7-1297-2014
- 404 Koutroulis, A.G., Grillakis, M.G., Daliakopoulos, I.N., Tsanis, I.K., Jacob, D., 2016. Cross sectoral
405 impacts on water availability at +2°C and +3°C for east Mediterranean island states: The
406 case of Crete. *J. Hydrol.* 532, 16–28. doi:10.1016/j.jhydrol.2015.11.015
- 407 Kyselý, J., Plavcová, E., 2010. A critical remark on the applicability of E-OBS European gridded
408 temperature data set for validating control climate simulations. *J. Geophys. Res.* 115,
409 D23118. doi:10.1029/2010JD014123
- 410 Li, H., Sheffield, J., Wood, E.F., 2010. Bias correction of monthly precipitation and temperature
411 fields from Intergovernmental Panel on Climate Change AR4 models using equidistant
412 quantile matching. *J. Geophys. Res.* 115, D10101. doi:10.1029/2009JD012882
- 413 Maraun, D., 2016. Bias Correcting Climate Change Simulations - a Critical Review. *Curr. Clim.*
414 *Chang. Reports* 2, 211–220. doi:10.1007/s40641-016-0050-x
- 415 Maraun, D., Wetterhall, F., Ireson, A.M., Chandler, R.E., Kendon, E.J., Widmann, M., Brienen, S.,
416 Rust, H.W., Sauter, T., Themeßl, M., Venema, V.K.C., Chun, K.P., Goodess, C.M., Jones,
417 R.G., Onof, C., Vrac, M., Thiele-Eich, I., 2010. Precipitation downscaling under climate
418 change: Recent developments to bridge the gap between dynamical models and the end
419 user. *Rev. Geophys.* 48, RG3003. doi:10.1029/2009RG000314
- 420 Maurer, E.P., Pierce, D.W., 2014. Bias correction can modify climate model simulated
421 precipitation changes without adverse effect on the ensemble mean. *Hydrol. Earth Syst. Sci.*
422 18, 915–925. doi:10.5194/hess-18-915-2014
- 423 Nikulin, G., Bosshard, T., Yang, W., Bärring, L., Wilcke, R., Vrac, M., Vautard, R., Noel, T.,
424 Gutiérrez, J.M., Herrera, S., Others, 2015. Bias Correction Intercomparison Project (BCIP):
425 an introduction and the first results, in: EGU General Assembly Conference Abstracts. p.
426 2250.
- 427 Olsson, T., Jakkila, J., Veijalainen, N., Backman, L., Kaurola, J., Vehviläinen, B., 2015. Impacts
428 of climate change on temperature, precipitation and hydrology in Finland – studies using bias
429 corrected Regional Climate Model data. *Hydrol. Earth Syst. Sci.* 19, 3217–3238.
430 doi:10.5194/hess-19-3217-2015
- 431 Papadimitriou, L. V., Koutroulis, A.G., Grillakis, M.G., Tsanis, I.K., 2015. High-end climate change
432 impact on European water availability and stress: exploring the presence of biases. *Hydrol.*
433 *Earth Syst. Sci. Discuss.* 12, 7267–7325. doi:10.5194/hessd-12-7267-2015



- 434 Papadimitriou, L. V, Koutroulis, A.G., Grillakis, M.G., Tsanis, I.K., 2016. High-end climate change
435 impact on European runoff and low flows – exploring the effects of forcing biases. *Hydrol.*
436 *Earth Syst. Sci.* 20, 1785–1808. doi:10.5194/hess-20-1785-2016
- 437 Parker, D., Horton, B., 2005. UNCERTAINTIES IN CENTRAL ENGLAND TEMPERATURE 1878–
438 2003 AND SOME IMPROVEMENTS TO THE MAXIMUM AND MINIMUM SERIES. *Int. J.*
439 *Climatol.* 25, 1173–1188. doi:10.1002/joc.1190
- 440 Parker, D.E., Legg, T.P., Folland, C.K., 1992. A new daily central England temperature series,
441 1772–1991. *Int. J. Climatol.* 12, 317–342. doi:10.1002/joc.3370120402
- 442 Pierce, D.W., Cayan, D.R., Maurer, E.P., Abatzoglou, J.T., Hegewisch, K.C., Pierce, D.W.,
443 Cayan, D.R., Maurer, E.P., Abatzoglou, J.T., Hegewisch, K.C., 2015. Improved Bias
444 Correction Techniques for Hydrological Simulations of Climate Change*. *J. Hydrometeorol.*
445 16, 2421–2442. doi:10.1175/JHM-D-14-0236.1
- 446 Prein, A.F., Gobiet, A., Truhetz, H., Keuler, K., Goergen, K., Teichmann, C., Fox Maule, C., van
447 Meijgaard, E., Déqué, M., Nikulin, G., Vautard, R., Colette, A., Kjellström, E., Jacob, D.,
448 2015. Precipitation in the EURO-CORDEX 0.11° and 0.44°
449 0.44° simulations: high resolution, high benefits? *Clim. Dyn.* 46, 383–412.
450 doi:10.1007/s00382-015-2589-y
- 451 Rubino, M., Etheridge, D.M., Trudinger, C.M., Allison, C.E., Rayner, P.J., Enting, I., Mulvaney, R.,
452 Steele, L.P., Langenfelds, R.L., Sturges, W.T., Curran, M.A.J., Smith, A.M., 2016. Low
453 atmospheric CO₂ levels during the Little Ice Age due to cooling-induced terrestrial uptake.
454 *Nat. Geosci.* 9, 691–694. doi:10.1038/ngeo2769
- 455 Sharma, D., Das Gupta, A., Babel, M.S., 2007. Spatial disaggregation of bias-corrected GCM
456 precipitation for improved hydrologic simulation: Ping River Basin, Thailand. *Hydrol. Earth*
457 *Syst. Sci.* 11, 1373–1390. doi:10.5194/hess-11-1373-2007
- 458 Sippel, S., Otto, F.E.L., Forkel, M., Allen, M.R., Guillod, B.P., Heimann, M., Reichstein, M.,
459 Seneviratne, S.I., Thonicke, K., Mahecha, M.D., 2016. A novel bias correction methodology
460 for climate impact simulations. *Earth Syst. Dyn.* 7, 71–88. doi:10.5194/esd-7-71-2016
- 461 Teutschbein, C., Seibert, J., 2012. Bias correction of regional climate model simulations for
462 hydrological climate-change impact studies: Review and evaluation of different methods. *J.*
463 *Hydrol.* 456, 12–29. doi:10.1016/j.jhydrol.2012.05.052
- 464 Themeßl, M.J., Gobiet, A., Heinrich, G., 2011. Empirical-statistical downscaling and error
465 correction of regional climate models and its impact on the climate change signal. *Clim.*
466 *Change* 112, 449–468. doi:10.1007/s10584-011-0224-4
- 467



468 List of Figures

469 *Figure 1: The transfer function (heavy black line) between observed (bottom histograms) and*
470 *modelled (histograms on the left) for the reference period (1981-2010) is used to adjust bias of a*
471 *30-year moving window starting from 1981-2010 to 2068-2097. The rightmost plot shows the*
472 *residual histogram after bias correction. The change in the average correction (red mark) on the*
473 *TF in comparison to the reference period mean correction (square) is shown. The animated*
474 *version provided in the supplemental information shows the temporal evolution of the bias as the*
475 *30-year time window moves on the projection data. Data were obtained from ICHEC-EC-EARTH*
476 *r12i1p1 SMHI-RCA4_v1 RCM model of Euro-CORDEX experiment (0.11 degrees resolution)*
477 *simulation under the representative concentration pathway of RCP85, for the location Chania*
478 *International Airport (lon=24.08, lat=35.54). Observational data were obtained from the E-OBS*
479 *v14 dataset (Haylock et al., 2008) of 0.25 degrees spatial resolution.*

480

481 *Figure 2: MSBC methodology on temperature correction using linear functions (borrowed from*
482 *Grillakis et al., (2013); modified) in one of the data segments.*

483

484 *Figure 3: Mean temperature of the EOBS (first line) and for each RCM model (second line) for*
485 *the reference period 1951-2005. The long term average difference (DIFF) between individual*
486 *models and EOBS are shown in the third line. The last column shows the ensemble mean of each*
487 *line. Different color maps are provided for the MEAN panels (1st and 2nd line) and the DIFF (3rd*
488 *line). Lines 4, 5, 6 are similar to 1 2 and 3 but for standard deviation.*

489

490 *Figure 4: The 6-fold cross validation scheme with the calibration (C) and the validation (V) periods*
491 *of each fold. Each experiment (Exp) was replicated for all five RCM models.*

492

493 *Figure 5: a) annual averages of temperature of the raw model data, the observations and the bias*
494 *correction with and without the NM, for the calibration period 1850 – 1899 (solid lines) and the*
495 *validation period 1900-2005 (dashed). Probability densities of annual (c) and of daily means (d).*

496

497 *Figure 6: Mean surface temperature of the cross validation test. Panels a and b show the*
498 *ensemble mean of the 5 raw models data and the EOBS respectively. Panels c and d show the*
499 *ensemble mean of the 5 RCM models after the correction with and without the NM module*
500 *respectively, for the calibration periods' data. Panels e and f show the difference of the c and d*



501 *panels for the EOBS, respectively, Panels g to j are the same as c to f but for the validation*
502 *periods' data.*

503

504 *Figure 7: Ensemble long-term linear trend of the 5 RCM models' data. The trend is estimated on*
505 *the mean temperature (top) and the 10th (mid) and 90th (bottom) percentiles in annual basis.*
506 *The change in the corrected data trend relatively to the raw data trend is provided for the BC*
507 *(middle panels) and the BCNM data (right panels). All values are expressed as degrees per*
508 *century [$^{\circ}\text{C}/100\text{ y}$].*

509

510 *Figure 8: Average of standard deviations for the study domain, for the raw data (a), the BC (b)*
511 *and the BCNM (c) for the different models and the observations, in annual basis. Differences*
512 *between the raw and the bias corrected standard deviations are shown in (d) and (e). Plots (f)*
513 *and (g) correspond to the same data as (d) and (e), but normalized for their 1951-2005 mean.*

514

515 **List of Tables**

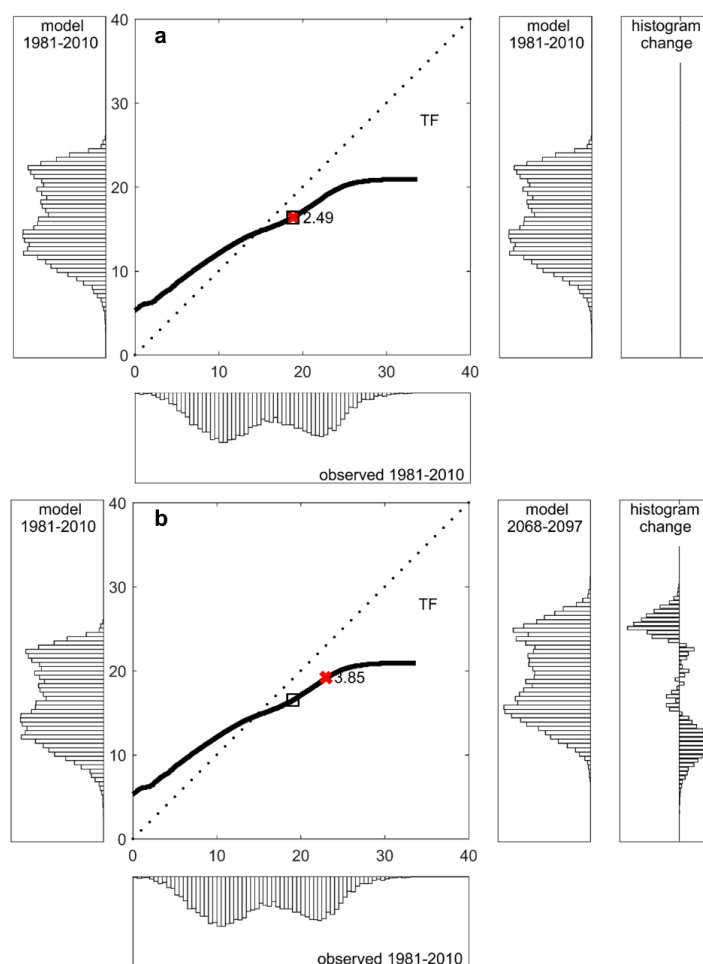
516 *Table 1: RCM models used in this experiment.*

517

518 *Table 2: Statistical properties of the calibration and the validation periods for the two bias*
519 *correction procedures. Variables denoted with * are estimated on annual aggregates. SD stands*
520 *for standard deviation and pn for the nth quantile.*

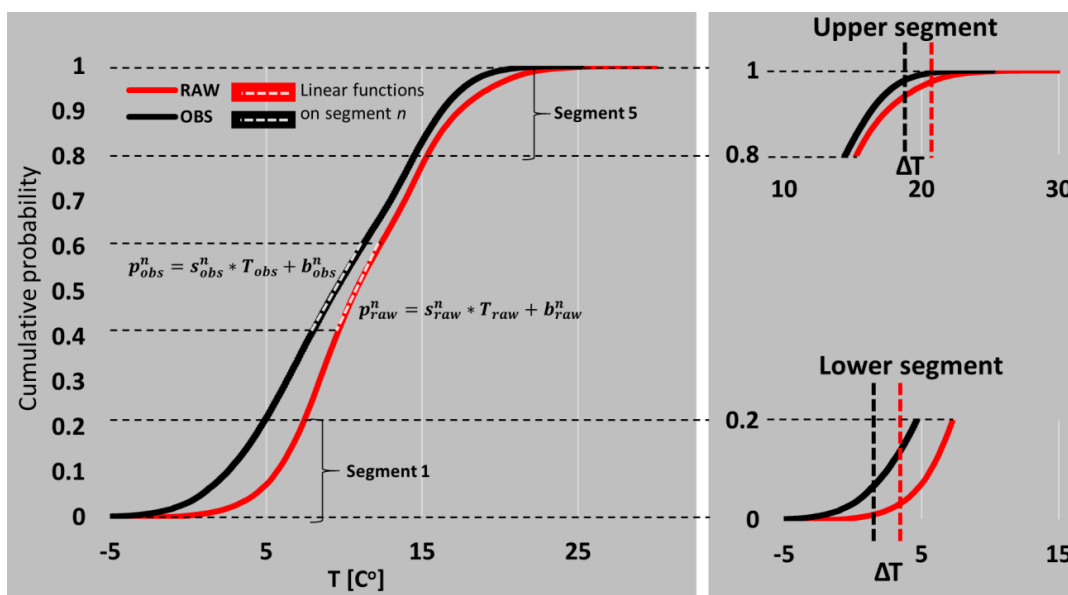
521

522



523
524
525
526
527
528
529
530
531
532
533
534
535

Figure 1: The transfer function (heavy black line) between observed (bottom histograms) and modelled (histograms on the left) for the reference period (1981-2010) is used to adjust bias of a 30-year moving window starting from 1981-2010 to 2068-2097. The rightmost plot shows the residual histogram after bias correction. The change in the average correction (red mark) on the TF in comparison to the reference period mean correction (square) is shown. The animated version provided in the supplemental information shows the temporal evolution of the bias as the 30-year time window moves on the projection data. Data were obtained from ICHEC-EC-EARTH r12i1p1 SMHI-RCA4_v1 RCM model of Euro-CORDEX experiment (0.11 degrees resolution) simulation under the representative concentration pathway of RCP85, for the location Chania International Airport (lon=24.08, lat=35.54). Observational data were obtained from the E-OBS v14 dataset (Haylock et al., 2008) of 0.25 degrees spatial resolution.

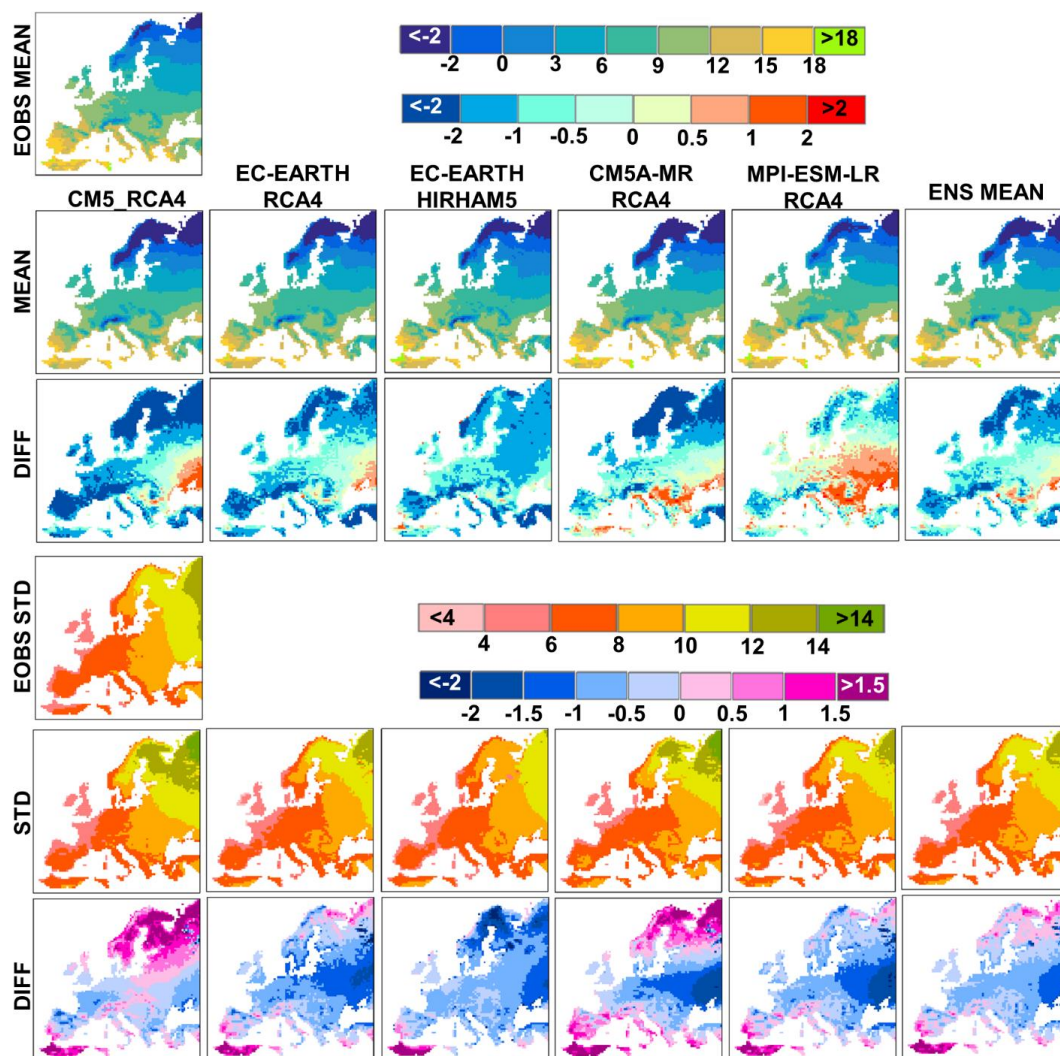


536

537

538

Figure 2: MSBC methodology on temperature correction using linear functions (borrowed from Grillakis et al., (2013); modified) in one of the data segments.



539
 540
 541
 542
 543
 544
 545

Figure 3: Mean temperature of the EObs (first line) and for each RCM model (second line) for the reference period 1951-2005. The long term average difference (DIFF) between individual models and EObs are shown in the third line. The last column shows the ensemble mean of each line. Different color maps are provided for the MEAN panels (1st and 2nd line) and the DIFF (3rd line). Lines 4, 5, 6 are similar to 1 2 and 3 but for standard deviation.



Fold	1	2	3	4	5	6
Exp 1	C	C	C	C	C	V
Exp 2	C	C	C	C	V	C
Exp 3	C	C	C	V	C	C
Exp 4	C	C	V	C	C	C
Exp 5	C	V	C	C	C	C
Exp 6	V	C	C	C	C	C
	1951-1960	1961-1970	1971-1980	1981-1990	1991-2000	2001-2010

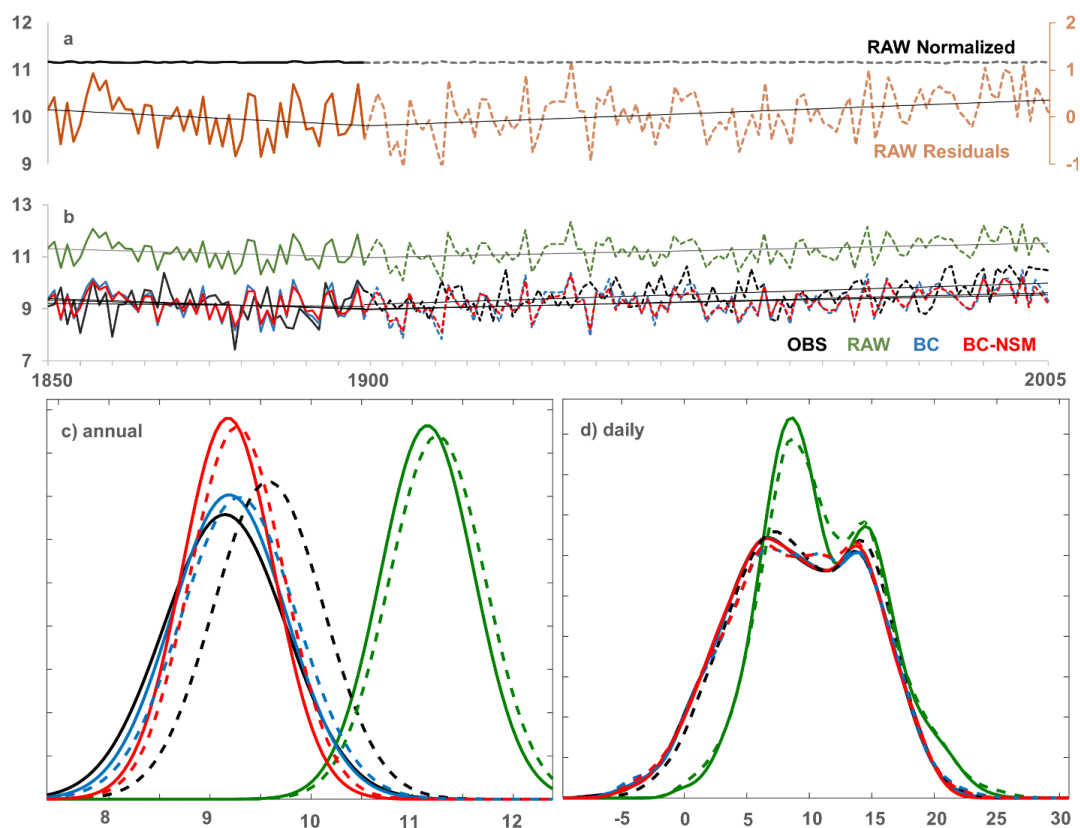
546

547

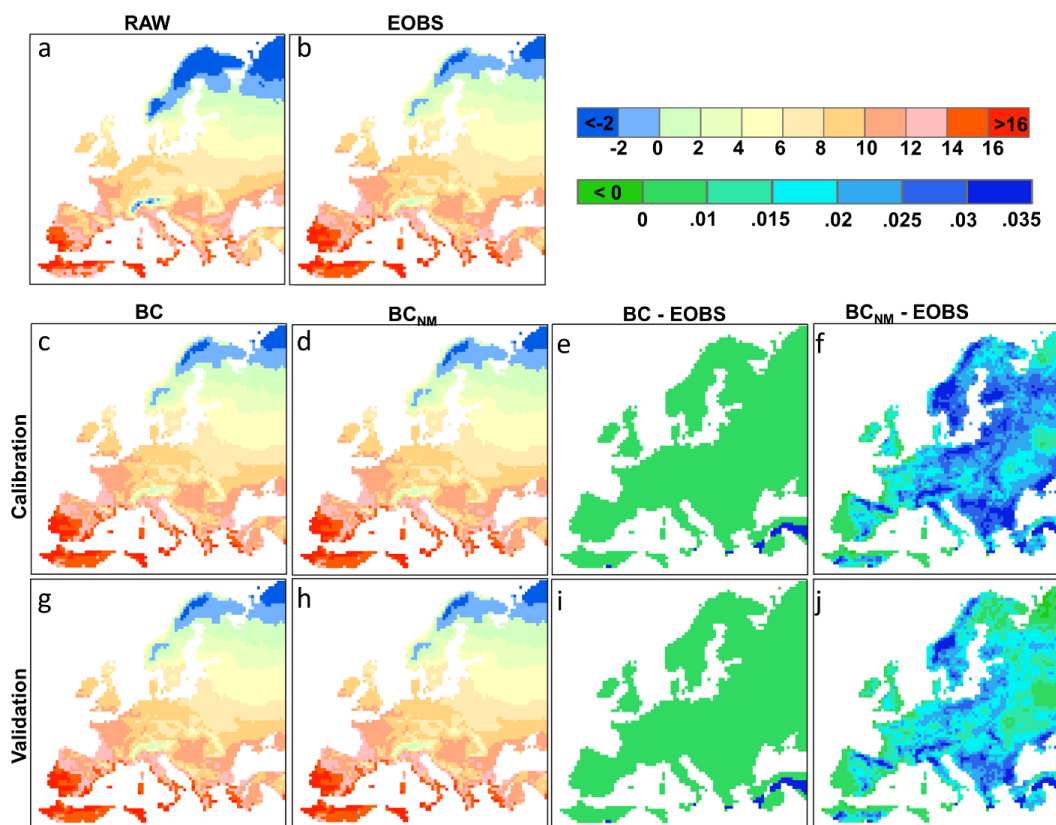
548

549

Figure 4: The 6-fold cross validation scheme with the calibration (C) and the validation (V) periods of each fold. Each experiment (Exp) was replicated for all five RCM models.

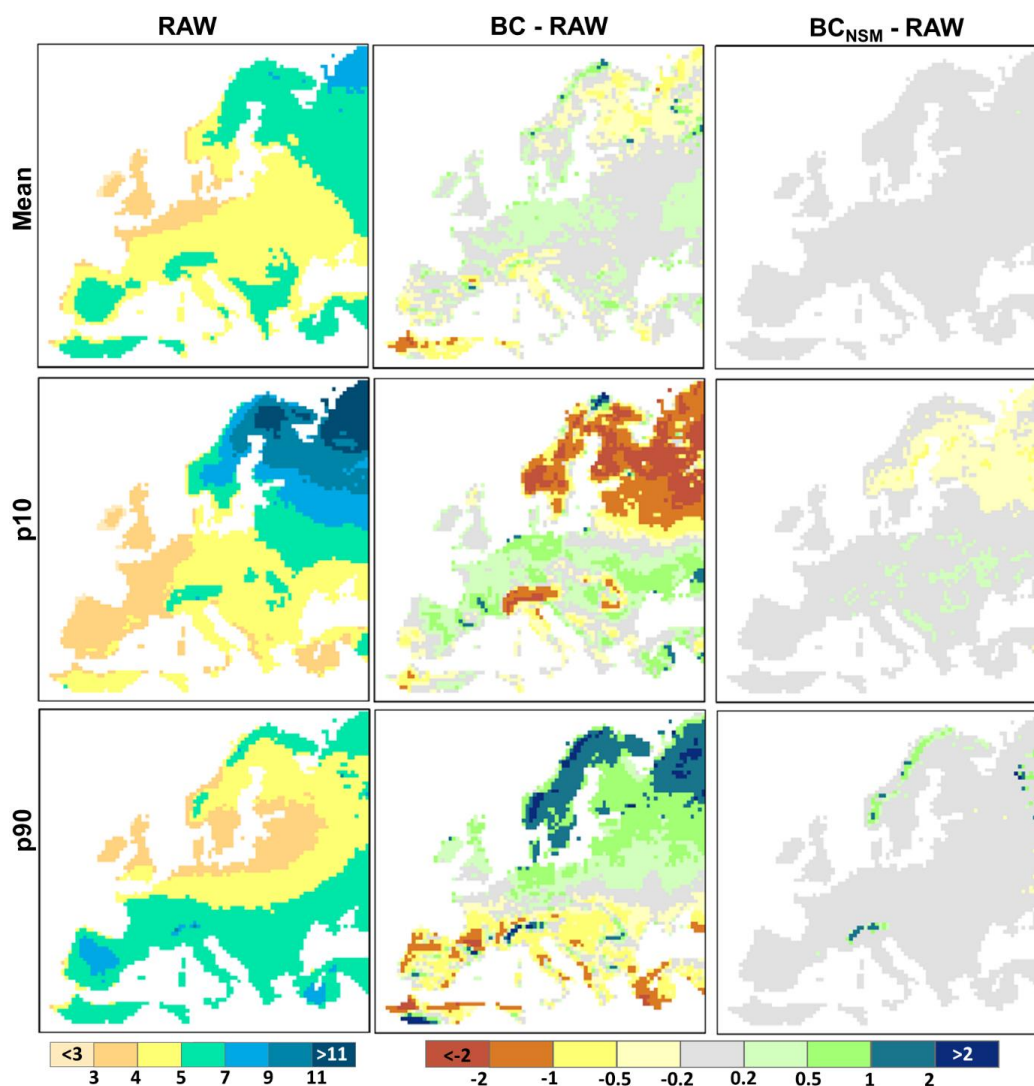


550
551 *Figure 5: a) annual averages of temperature of the raw model data, the observations and*
552 *the bias correction with and without the NM, for the calibration period 1850 – 1899 (solid*
553 *lines) and the validation period 1900-2005 (dashed). Probability densities of annual (c)*
554 *and of daily means (d).*
555



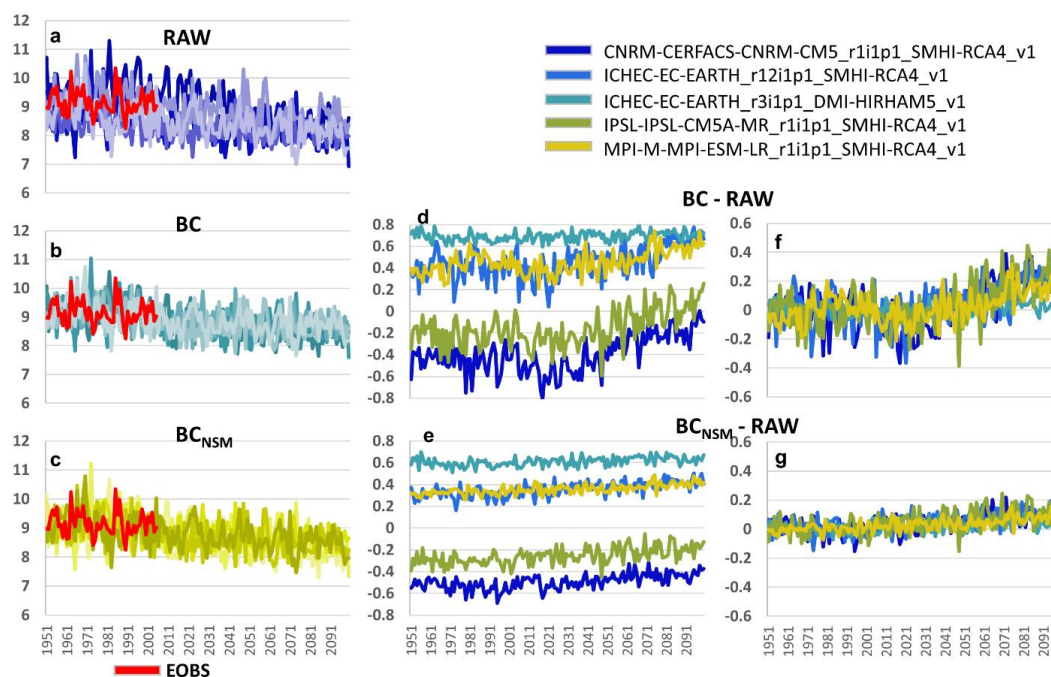
556
 557
 558
 559
 560
 561
 562
 563

Figure 6: Mean surface temperature of the cross validation test. Panels a and b show the ensemble mean of the 5 raw models data and the EOBS respectively. Panels c and d show the ensemble mean of the 5 RCM models after the correction with and without the NM module respectively, for the calibration periods' data. Panels e and f show the difference of the c and d panels for the EOBS, respectively, Panels g to j are the same as c to f but for the validation periods' data.



564
 565
 566
 567
 568
 569
 570
 571

Figure 7: Ensemble long-term linear trend of the 5 RCM models' data. The trend is estimated on the mean temperature (top) and the 10th (mid) and 90th (bottom) percentiles in annual basis. The change in the corrected data trend relatively to the raw data trend is provided for the BC (middle panels) and the BCNM data (right panels). All values are expressed as degrees per century [$^{\circ}\text{C}/100$ y].



572
 573
 574
 575
 576
 577

Figure 8: Average of standard deviations for the study domain, for the raw data (a), the BC (b) and the BCNM (c) for the different models and the observations, in annual basis. Differences between the raw and the bias corrected standard deviations are shown in (d) and (e). Plots (f) and (g) correspond to the same data as (d) and (e), but normalized for their 1951-2005 mean.



578

Table 1: RCM models used in this experiment.

#	{GCM}_{realization}_{RCM}
1	CNRM-CM5_r1i1p1_SMHI-RCA4_v1
2	EC-EARTH_r12i1p1_SMHI-RCA4_v1
3	EC-EARTH_r3i1p1_DMI-HIRHAM5_v1
4	IPSL-CM5A-MR_r1i1p1_SMHI-RCA4_v1
5	MPI-ESM-LR_r1i1p1_SMHI-RCA4_v1

579

580



581 **Table 2: Statistical properties of the calibration and the validation periods for the two bias**
 582 **correction procedures. Variables denoted with * are estimated on annual aggregates. SD stands**
 583 **for standard deviation and pn for the nth quantile.**

	Parameter	RAW	Normalized	Residuals	OBS	BC	BC _{NM}
Calibration	Slope [°C/10yr]*	-0.067	0.000	-0.067	-0.026	-0.086	-0.065
	Mean [°C]	11.2	11.2	0.0	9.1	9.2	9.2
	SD [°C]	4.5	4.6	0.9	5.3	5.3	5.3
	p10 [°C]	5.7	5.7	-0.9	2.1	2.2	2.2
	p90 [°C]	17.4	17.2	1.0	16.3	16.3	16.2
Validation	Slope [°C/10yr]*	0.052	0.000	0.051	0.076	0.062	0.051
	Mean [°C]	11.3	11.2	0.1	9.6	9.3	9.3
	SD [°C]	4.7	4.6	0.9	5.2	5.5	5.4
	p10 [°C]	5.6	5.7	-0.9	2.7	2.0	2.0
	p90 [°C]	17.4	17.2	1.0	16.3	16.3	16.2

584

585